Available online at www.sciencedirect.com

ScienceDirect

Procedia CIRP 34 (2015) 212 – 216

www.elsevier.com/locate/procedia

9th International Conference on Axiomatic Design – ICAD 2015

Momentary Local Laser Heating in Thermal Roll-to-Plate Nanoimprinting; Node Decoupling with Axiomatic Design

Masayuki Nakao[a*], Ken Takahashi[a], Keisuke Nagato[a], Kenji Iino[b]

a Department of Engineering Synthesis, School of Engineering, The University of Tokyo, Hongo7-3-1, Bunkyo-ku, Tokyo, Japan
b SYDROSE LP, 475N. 1st St., San Jose, CA95112, USA

* Corresponding author. Tel.: +81-3-5841-6360; fax: +81-3-5800-6997. E-mail address: nakao@hnl.t.u-tokyo.ac.jp

Abstract

The independence axiom of axiomatic design to decouple interference among functional requirements might be effective in designing new processes. This paper reports an application of this concept to our design of roll-to-plate thermal nanoimprinting using laser heating. The authors, instead of heating an entire roller, casted a laser beam through a glass roller to a thin metal film on the mold to produce a momentary and local heat source. The mold immediately cooled down after the laser heating and the patterned resin did not reflow back to flat shapes; we succeeded in decoupling the node of heating and cooling.

Peer-review under responsibility of the organizing committee of 9th International Conference on Axiomatic Design

Keywords: Decouple; Laser; Nanoimprinting

1. Introduction

1.1 Axiomatic design application in product and process design

After Suh introduced axiomatic design in 1990 [1], it has been applied in a number of design analyses of products and processes. The method is to apply the independence axiom to select the Design Parameter (DP) vector to remove interferences among Functional Requirements (FR), and then to apply the information axiom to optimize the DP vector to maximize the sum of the probability of success for each functional requirement. At the same time, the DP vector has to satisfy the Constraints (C) as a boundary condition of DPs, e. g., cost, life, lead time, rigidity, or system efficiency [2]. Figure 1 shows the relation between the FR and DP vectors with the Design Matrix (DM). The DM of a coupled design is "non-diagonal" with non-zero non-diagonal components; however, "decoupling", i.e., removing interferences with some new DPs will make all non-diagonal components of the matrix zero, and thus the matrix turns diagonal. The Cs are expressed by linear relations of the DP vector.

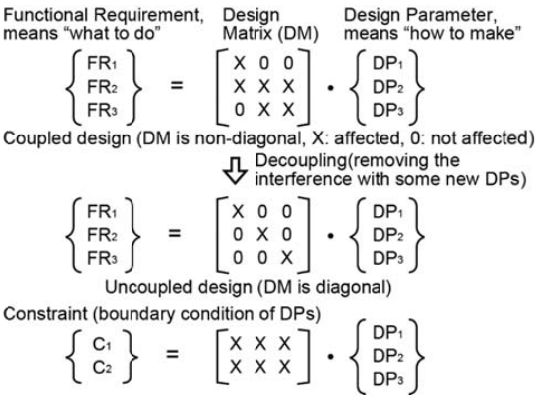

Fig. 1. Decoupling in Axiomatic Design.

Peer-review under responsibility of the organizing committee of 9th International Conference on Axiomatic Design
doi:10.1016/j.procir.2015.07.001

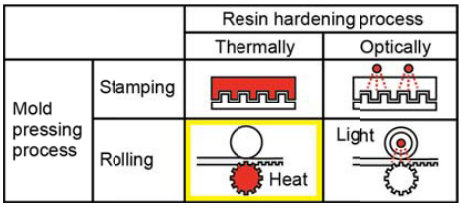

Fig. 2. Categories of nanoimprinting.

Note that products and processes have a large number of functional requirements [3]. When the number of FRs is 20, for example, we have to check the interferences for 20x20=400 cases, and such a strict analysis burdens the designer. From our experience, keeping the number of FRs to 5 or less, is quite effective to keep the designer concentrated on important FRs. For this paper, we excluded FRs with success rates of 1 or 0, meaning those are always or never accomplished, and set n=3.

1.2 Designing the nanoimprinting process

Chou reported nanoimprinting in 1995 [4]. The process produces geometric patterns of about 30nm width on silicon and replicates the inverse pattern on resin by pressing. The resin is then used for masks. A number of researches have been since then advancing the process. Figure 2 shows the 4 groups of these follow-up studies. First, they are divided into 2 groups based on whether the resin is hardened "thermally" by cooling thermoplastic resin after heating, softening and pressing it against a patterned mold, or "optically" by putting photo-curing resin, in the form of liquid or powder, under light after is has been pressed against a metal mold. The second categorization distinguishes between "stamping" and "rolling" the metal mold. Altogether the 2x2 categorizations define 4 types. The optically hardening process proceeds under room temperature, thus it eliminates the need for thermal design; however, the photo-curing resin costs about 10 times higher price of thermoplastic resin. Rolling is a

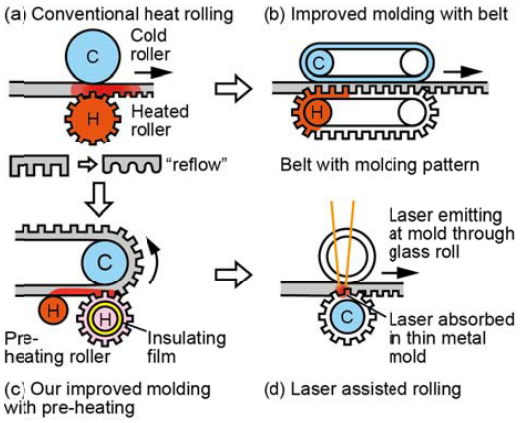

Fig. 3. Thinking process of decoupling in rolled thermal nanoimprinting.

widely used process in metal rolling or paper printing. The process control is demanding with short time and localized area when the roller and sheet come in contact; however, rolling has advantage in its about 10 times faster process time than stamping.

The process we developed and report in this paper is in the lower left-hand corner of Figure 2, i.e., rolling and thermal nanoimprinting. Among the four, this process is most likely to have the lowest production cost and is suited for production of out-coupling film for organic electroluminescence displays or anti-reflection film for liquid crystal television screens.

2. Axiomatic design of a laser assisted roll-to-plate thermal nanoimprinting

2.1 Records of our thinking process to accomplish decoupling

Figure 3 (a) shows a conventional roll-to-plate thermal nanoimprinting. For this conventional system of replicating nano-structures on the roller mold to the resin sheet, processes for heating, pressing, cooling, and mold releasing have to be implemented near the contact area of the roller and sheet. Past methods of using a metal roller with a heater for raising the resin sheet temperature succeeded in softening the resin and replicating the mold patterns; however, the metal roller remained hot. The resin sheet then is released from the mold before cooling down to a temperature of the glass transition point (Tg), and the surface tension in the still soft patterns would reflow the resin back to flat shapes. Axiomatic design explains this phenomenon as interference between the heating and cooling processes.

For the purpose of better understanding reflow, we put 4 types of resin sheet through stamping thermal nanoimprinting processes. Figure 4 shows the ratios of the replicated form heights to that of the metal mold (replication ratios). The mold has an array of hemispheres of 15μm in height and 30μm in diameter. The larger feature is more difficult to be replicated because it needs larger heating value. As the upper figure shows, each type of resin flows better with higher mold temperature and higher mold pressure. The lower figure shows that the mold temperature upon mold release caused

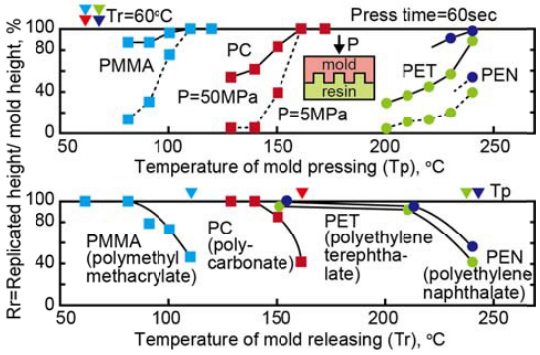

Fig. 4. Replication ratio (Rr) in stamping thermal nanoimprinting with four types of resin.

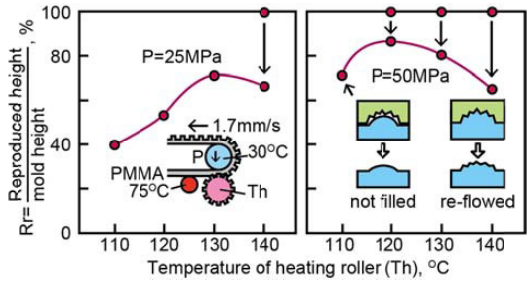

Fig. 5. Replication ratio (Rr) in rolling thermal nanoimprinting.

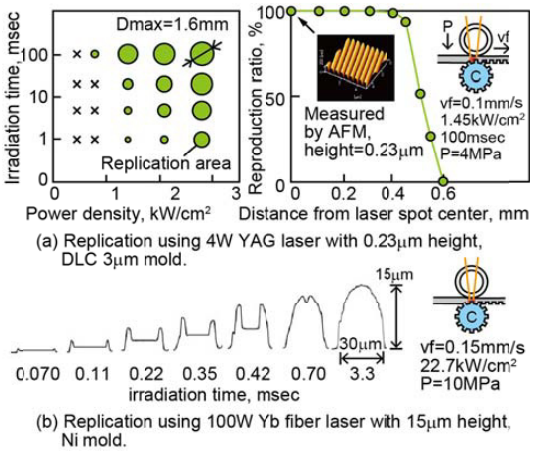

Fig. 6. Ratio of replication in laser heated rolling thermal nanoimprinting.

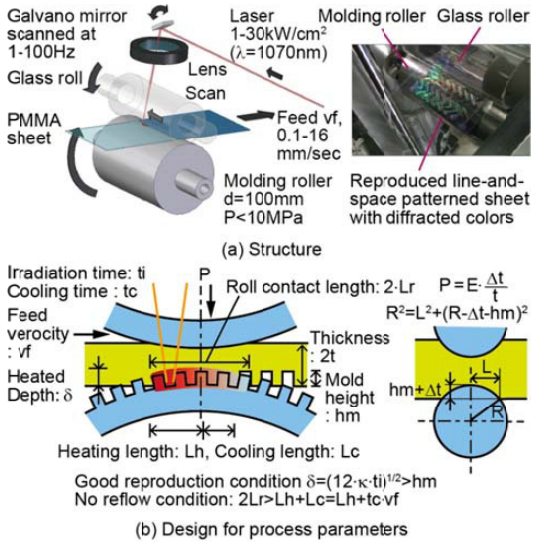

Fig. 7. Process design for laser heated rolling thermal nanoimprinting.

reflow when it was above Tg, resulting in lower replication ratio. This experiment demonstrated that the above interference takes place no matter what the resin was.

Figure 3 (b) shows the improved system Ogino developed [5]. The mold was given a belt shape, instead of a roller shape, to have a longer cooling area after the heating area. This belt-shaped thick nickel plated mold for high tension, however, turned out to be expensive and did not meet the cost constraint.

Figure 3 (c) shows our improving configuration with a pre-heating roller to lessen the amount of heat input at the roller contact point; so the resin sheet can quickly go into its cooling process. This trial, however, resulted in necking with elongation in the rolling direction and shrinking in the lateral by the sheet tension of 0.8MPa. We observed this necking when the pre-heating temperature was around Tg, 110°C for polymethyl methacrylate (PMMA). Yet another attempt we made to cool the mold quickly placed a heat insulating polyimide sheet of 250μm thick between a thin nickel film on the roller surface and the roller body inside. For better cooling of the resin sheet, we wrapped the resin sheet halfway around the cooling roller.

As Figure 5 shows, the replication rate reached as high as 83% with higher mold temperature and higher mold pressure; however, when the mold temperature exceeded a certain point, reflow caused a drop in the replication ratio (Rr). For this case, the replicated ridges had dimples of size about 1μm. These dimples from the metal mold were a sign of a 100% Rr when the resin contacted the metal mold. The lowered Rr after the entire process was a sign that reflow caused the ridges to reduce their heights. The heating and cooling processes were still interfering.

Figure 3 (d) shows our last attempt which is the subject of this paper. We produced a glass roller to pass a laser beam to cast on the contact area where the laser is absorbed to the metal mold. The laser wavelength was 1.07μm, and the absorption rate was 0% for glass and PMMA, 28% for nickel, 50% with a 0.1μm diamond-like carbon (DLC) layer on the nickel, and 90% with a 3μm DLC layer on it. Figure 6 (a) shows the results using 0.23μm height mold with 3μm DLC and 4W YAG laser [6]. The diagram on the left shows the replication area with intermittent laser irradiation. The area was larger with greater laser power density and longer irradiation time. The replication area, as the diagram on the right shows, accomplished a Rr of 100% free of reflow in the center. Figure 6 (b) shows the results using 15μm height Ni mold replicate a higher hemisphere. Deformation speed was 10-40 μm/msec at 10 MPa. Irradiation time of 3.3msec could make a Rr of 100% without reflow.

Figure 7 (a) shows the outline of the experiment setup. Figure 7 (b) shows how we set the process parameters. First the heated depth (δ) had to be larger than the metal mold feature height (hm) for proper replication. Solving the 1 dimensional heat transfer problem for finding the δ, we have [12 x (resin thermal diffusivity κ: 1.0 x $10^{-7}m^2/s$) x (irradiation time: 3msec)] ^0.5=60μm. The maximum hm for our molds was 15μm, less than 60μm; thus replication was feasible. Also, to prevent reflow, we will keep the roll contact length (2·Lr) longer than the sum of the heating length (Lh) and the cooling lengths (Lc). The Lh, for example, was the

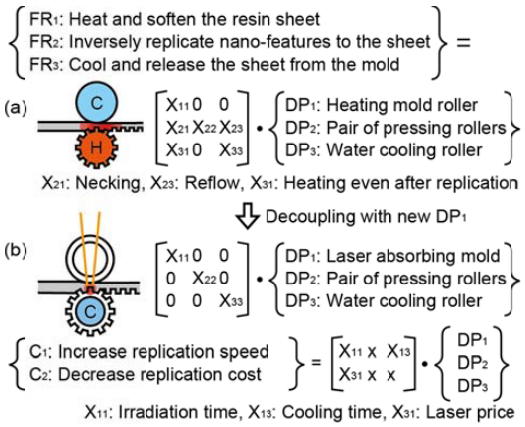

Fig. 8. Design equation of laser heating in rolling thermal nanoimprinting.

laser spot diameter of 0.5mm with a power density of 23kW/cm^2 and an irradiation time of 3msec. A temperature transition simulation gave a cooling time of 5msec for this example. Multiplying this 5msec to the feed velocity of 16mm/s resulted in Lc=0.08mm. The 2·Lc, on the other hand, for conditions of 10MPa mold pressure, 2GPa Young's modulus of resin, 75μm sheet thickness, 15μm mold height, and 100mm roller diameter, came out to be 1.2mm as shown in Figure 7 (b). This length of 1.2mm prevented reflow because this 1.2mm is larger than the sum of Lh=0.5mm and Lc=0.08mm.

A galvano mirror scans the 100W laser in the lateral direction. To replicate seamlessly by scanning the spot in the range of 100mm, the feed velocity (vf) should become slower to 0.83 mm/s under the irradiation time (ti) of 3msec. If we can shorten ti to 0.15msec with a higher power laser, we can get a larger vf of 16mm/s and a shorter heated depth (δ) of 13μm, requiring a DLC layer for higher absorption. Consequently, vf, ti, and δ have interferes; so we define vf as a constraint in next section.

2.2 Decoupling interference with laser heating

Figure 8 shows the design equations for conventional rolling thermal nanoimprinting in Figure 3 (a) and laser assisted heating in (d). We set the functional requirements to; FR_1: Heat and soften the resin sheet, FR_2: Inversely replicate nano-features to the sheet, FR_3: Cool and release the sheet from the mold. Figure 8 (a) shows the design parameters of the conventional one; DP_1: Heating mold roller, DP_2: Pair of pressing rollers, DP_3: Water cooling roller. Interferences were, as we explained above, X_{21}: Necking, X_{23}: Reflow, and X_{31}: Heating even after replication, these interferences make the DM non-diagonal. For the laser heated case of Figure 8 (b), the FRs were the same, but with a different DP_1: Laser absorbing mold, the FRs were decoupled to make the DM diagonal. We succeeded in rolling thermal nanoimprinting with a 100% replication ratio.

Constraints were; C_1: Increase replication speed, and C_2: Decrease replication const. Rough values for these constraints were C_1: 1m/min=16mm/s or faster, and C_2: 10$/m^2 or lower. These constraints were both affected by DP_1, DP_2 and DP_3; the replication speed C_1 was strongly affected with the irradiation time DP_1 and cooling DP_3, and the production cost C_2 strongly with the fiber laser price for DP_1.

3. Discussion

This section reports the results of applying the decoupling method of process design using the same fiber laser to the other processes, that is, laser welding and laser cladding. The following results are from interviews we conducted to the designers to verify decoupling of interferences.

3.1 Decoupling interference with laser welding

Figure 9 shows the design equations for (a) conventional spot welding and (b) new laser welding. For realizing the functional requirements FR_1: Make the plates contact each other, FR_2: Melt the plates around the contact spot, and FR_3: Increase the welding area, conventional spot welding (a) selected design parameters DP_1: Clamping tool, DP_2: Electric resistance welding, DP_3: Pitch of welding spots. Interferences for this case are X_{21}: Requires clamping tool to pass electricity, X_{23}: Narrower pitch of spots disables welding due to current leakage to adjacent welded spots, and X_{31}: Places that cannot be clamped by the tools cannot be welded. Higher rigidity with a narrower spot pitch would cause electricity leakage, i.e., added spots and electricity leakage interferes.

Laser welding in case of (b) has the same set of functional requirements to realize. Changing the design parameters to DP_1: Crimping or temporary welding and DP_2: Plug welding with laser leads to a design equation that shows successful decoupling of interference. The clamping tool for (a) occupies areas on both sides of the plates; however, tools for laser beaming only sit on one side. Heat input with laser is also

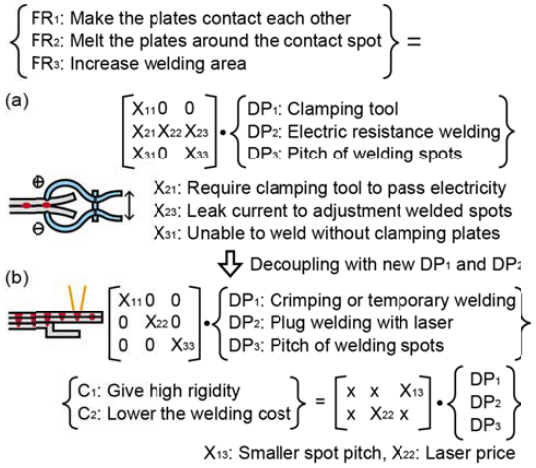

Fig. 9. Design equation of laser welding.

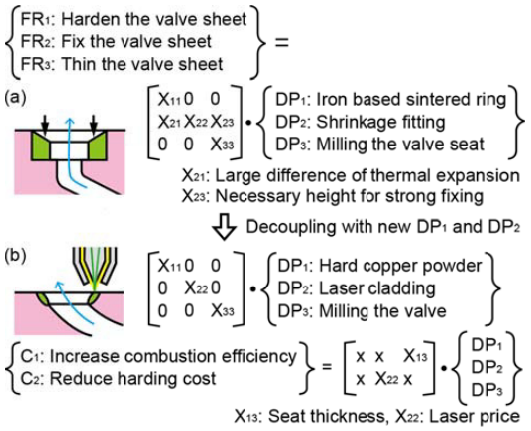

Fig. 10. Design equation of laser cladding.

narrowly localized and the spot weld pitch is small. The constraints for this case are C_1: Give high rigidity, and C_2: Lower the welding cost. A smaller spot pitch with DP_3 strongly affects the rigidity C_1 and the fiber laser price for DP_2, the cost C_2.

3.2 Decoupling interference with laser cladding

Figure 10 shows that conventional valve seats for an aluminum engine block use (a) press inserted sintered rings. For a new design, they are replaced with (b) laser cladding. Thinner this seat is, intake to the engine makes a low angle flow that generates better swirling to increase the combustion efficiency of engines. The functional requirements are; FR_1: Harden the valve seat, FR_2: Fix the valve seat, and FR_3: Thin the valve seat. For case (a), the design parameters are; DP_1: Iron based sintered ring, DP_2: Shrinkage fitting and DP_3: Milling the valve seat. The DM shows interferences of X_{21}: Strong pressing required for compensating the difference of thermal expansion, and X_{23}: Strong fixing requires certain height while a thinner seat is desired. For this case, seat thickness and fixing strength interfere.

The new design in this case selects laser cladding. Case (b) has the same set of FRs, however, a different set of design parameters; DP_1: Hard copper powder, and DP_2: Laser cladding. The change realizes a strong surface yet with a thin seat and the combustion efficiency goes up by several percent. The DM is diagonal showing a successful decoupling of interference. The constraints are C_1: Increase the combustion efficiency, and C_2: Reduce the hardening cost. The swirling of C_1 is affect by the seat thickness DP_3, and cost C_2 by the fiber laser price DP_2.

4. Conclusion

In designing a new process, applying the independence axiom of axiomatic design effectively led to a design solution with decoupled functional requirements. This paper reported our analysis with laser heated roll-to-plate thermal imprinting, laser welding, and laser cladding. For each case, there existed interferences of, respectively, heating and cooling, added spots and electricity leakage, and seat thickness and fixing strength. We showed for these cases that momentary local laser casting succeeded in decoupling the interferences innovatively.

References

[1] Suh, N. P., 1990, The Principles of Design, Oxford University Press.
[2] Brown, C. A., 2014, Axiomatic Design of Manufacturing Processes Considering Coupling, Proceedings of the Eighth International Conference on Axiomatic Design, 149-153.
[3] Thompson, M. K., 2013, Improving the requirements process in Axiomatic Design Theory, Annals of the CIRP 62(1): 115-118.
[4] Chou, S. Y., Krauss, P. R., Renstrom, P. J., 1995, Imprint of sub-25 nm vias and trenches in polymers, Applied Physics Letters, 67-21: 3114-3116.
[5] Ogino, M., Hasegawa, M., Sakane, K., Nagai, S., Miyauchi, A., 2008, Fabrication of 200-nm Dot Pattern on 15-m-Long Polymer Sheet Using Sheet Nanoimprint Method, Japanese Journal of Applied Physics, 52: 035201.
[6] Nagato, K., Takahashi, K., Sato, T., Choi, J., Hamaguchi, T., Nakao, M., 2014, Laser assisted replication of large area nanostructures, Journal of Materials Processing Technology, 214: 2444-2449.